Discussions on Resolution of Different TDEM Survey Techniques for Detecting Water-Bearing Structures

Lei Yang
Dept of Xin Jiang Geology Exploration
No. 203 Research Institute of CNNC
Xian Yang, P.R.C

R.W.Groom
Principal
Petros Eikon Incorporated
Orangeville, Ontario, Canada

Abstract-*It is common when using TDEM to measure only inside the transmitter loop. In groundwater and environmental applications, this is almost ubiquitous. This situation arose, historically, as inversion applications only were available for central loop readings (Anderson, 1993) and geoscientists thought of such readings as soundings similar to resistivity sounding applications. But, should we consider TDEM data as analogous to reflection data and measure proximate to the source or as analogous to refraction data and measure away from the source? In mining applications, three-dimensional modeling has long been available and the use of multiple measurements inside and outside loops has been common for three decades. In this paper, we examine several misunderstandings and problems associated with inloop approaches by comparing results from different TDEM survey techniques. We utilize both synthetic and field data for our studies.*

Both synthetic and field data indicates that the use of in loop data is potentially dangerous as this location is poor for sensing the resistivity structure. In addition, single station inversion is limited without considerable geological knowledge as 1D inversion is highly non-unique. The use of multiple data in a 1D inversion helps locate the correct model subspace and it appears that out-of-loop data has fewer possible models. Fixed loop surveys can provide more accurate deep inversion results if the ground is sufficiently one-dimensional while also providing for faster surveys and more survey coverage.

Key Words: TDEM Survey Techniques; modeling; Decay Curve analysis; Water-Bearing Structure.

I. INTRODUCTION

A TDEM system induces currents in conducting earth (Faraday's law) and these currents migrate outwards and downwards with increasing time after the current is varied or turned off. These currents move outside the loop and downwards away from the transmitter and thus if the sensor is position inside the loop, it is further and further from the current concentrations as time progresses. We suggest that the receivers outside the loop should be more sensitive to the deeper rocks and soils as they are closer to concentrations of the migrating currents beneath the surface thus providing better resolution of variable layers beneath the earth. The rate of migration is determined by the resistivity of the soils and rocks. In very resistive environments these current concentrations are not observed except in very early time and thus the more resistive the ground, the poorer is the results of the inloop inversions.

II. CURRENT MIGRATION SYNTHETIC STUDIES

For this study, we are considering zones of unconsolidated sediments particularly to finding a saturated sandstone layer. The unconsolidated rocks are underlain with more consolidated, resistive rocks. This model is representative of our field site. The instrumentation utilized here will be fairly standard. We utilize a small loop, 100m by 100m; a bipolar current waveform with an approximate linear turn-off (ramp) and measurements of the time varying magnetic field in the off-time. In this study, the instrumentation utilizes coils to measure the voltage and thus dB/dt is sensed by the antenna. However, most conclusions are unaffected by measurement with a magnetometer. In our examples, we utilize a 25Hz base frequency as this serves to illustrate all of our points. We will utilize fairly standard time windows with no particularly early windows so as not to overcomplicate the analyses with bandwidth issues. Forward modeling algorithms use standard frequency domain simulations (e.g. Anderson 1975&1982, Boerner, 1984 and Johansen and Sorensen, 1979) with a non-standard band limited frequency to time transformation (Groom, 2000) which is more representative of the typical instrument's system response.

We simulate the horizontal components of the electric field (Ex, Ey) at a depth of 200m in the 6 Ωm clay zone using our standard model (Fig 4). We display the total current density as a function of horizontal position at this depth for a current in the loop of 25A. Figure 1 shows current migration at a time of 2.2msec after the end of the ramp (0.4msec). We see from this figure that the areas of largest current concentration are outside the loop and thus the total current underneath the loop and within the clay zone is small. When attempting to resolve this layer, receivers at a distance of approximately 200m from the centre would be more useful.

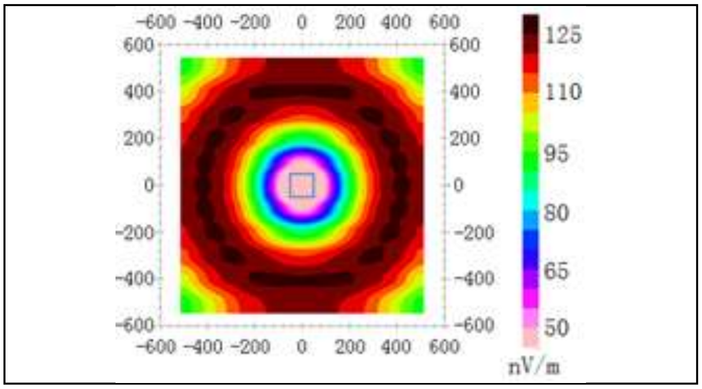

Fig. 1. Currents at mid-time at z=200

In Figure 2, the migrations are observed by displaying Hz at ground level as amplitude surfaces at different times. Figure 2(a) represents the current waveform, figures 2(b), 2(c) and 2(d) map the early, intermediate and late time current migration. We can observe that at early times the induced currents are concentrated near the loop but by late time, they are now distributed over a very large region.

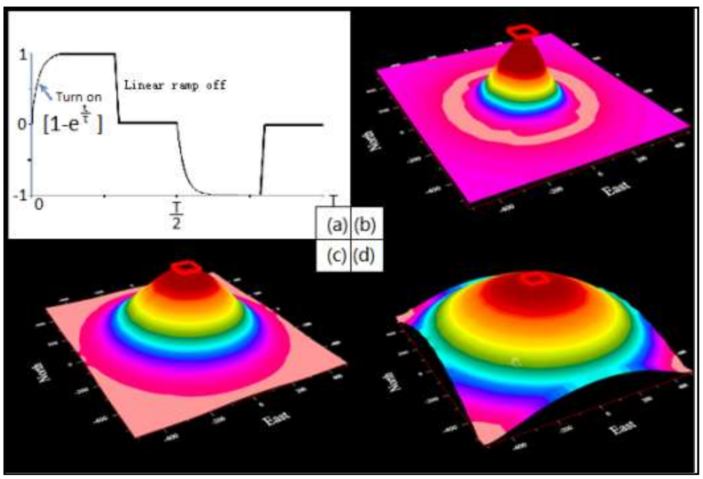

Fig. 1. Current migration underground reflected in a surface of Hz

Figure 3 displays the total horizontal current as a function of depth for the standard model below two positions, one inside the loop and one outside the loop. Figure 3(a) shows these fields at the very earliest of channels, figure 3(b) shows these fields at channel 15. The red curve plots the total electric field in mV/m below a point 25m east of the centre of the loop and the blue curve the same field but below a point 200m east of the center of the loop.

At early time, the electric fields are concentrated near the surface and closer to the centre of the loop but late early time (2 msec), the electric fields and thus the currents have migrated down to be concentrated in the conducting zone between (45m and 245m) but also outwards so that the currents at 200m are a full order of magnitude greater than those below the loop. For a measurement inside the loop for inversion purposes, these enhanced currents at a distance are not of great use in resolving deeper layers.

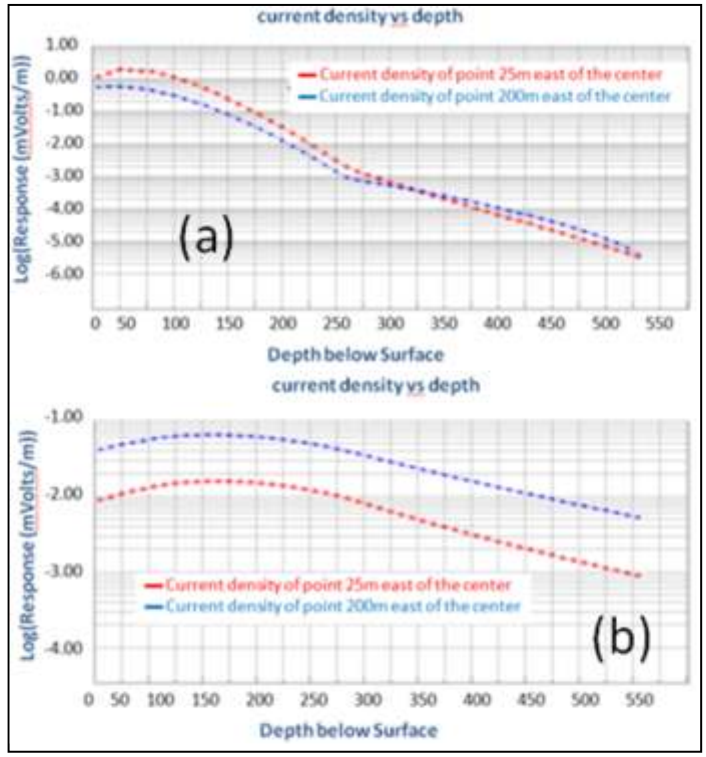

Fig. 2. Total horizontal Voltage below an inside and outside station

III. Simulation Result Comparison

Figure 4(a) shows the basic model that we utilize for this study. Figure 4(b) shows the response decay for a central loop coil receiver due to the model and the waveform described and normalized to current. Figure 4(c) is a comparison between the response of our full model, the response (blue) when the 3rd layer is infinite and the response (green) when the 4th layer is infinite.

With this comparison, we learn that the simulated data with an in-loop configuration cannot clearly distinguish the character of the basement, and without an excellent a prior starting model, the basement is difficult to discriminate. This model at later time with lower base-frequency will stretch the dynamic range even further. Even at 25Hz base frequency, the response covers 3 decades of amplitude which is hard for most commercial equipments to reproduce such a dynamic range.

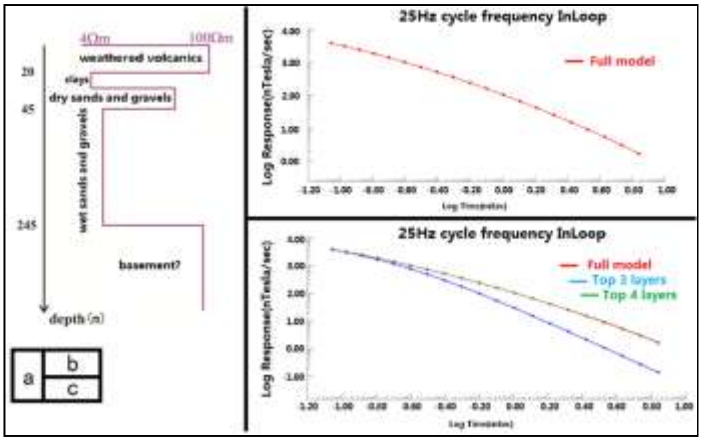

Fig. 3. Comparison of in-loop data from standard model vs similar models

Figure 5 is a comparison of different inversion results calculated from the in-loop data. Figure 5(a) is a 5 layer over a half space inversion (Jia and Groom, 2005) with no constraints using only a half space as the starting model. The blue data line is the simulation of the inversion model shown below the plot but utilizing only the top 3 layers of the inversion. This demonstrates at least 3 models which have identically the same response. Figure 5(b) is a multi-layered Occam inversion (Jia and Groom, 2005) starting with a half space. Again, we have another model with precisely the same response but again little resolution of actual structure. Figure 5(c) is an entirely different approach. We assume that we have some knowledge of the structure but not the true thicknesses or resistivities. Thus, we utilize a starting model which has alternating resistive and conducting layers. The blue curve is the response of the starting model. It does not have the same amplitude but does have a very similar decay pattern as the true model. The derived inversion model is shown in green and it is quite close to the true model. There were no constraints applied other than the number of layers. This can be described as a case of sampling the starting model from the correct model subspace.

All curves from different inversions above can fit the original curve reasonably well, but only with an a starting model which is approximately the correct structure can we produce a result which is close to the real situation underground. From this experiment, we can see that a single position and separation has multiple possible models particularly with data centered on the loop. Without the use of geological control to constrain the model, we cannot derive the correct model. As demonstrated, smooth over-parameterized inversions do not provide accurate estimations of resistivity or depths but only a rather unfocussed image of the ground.

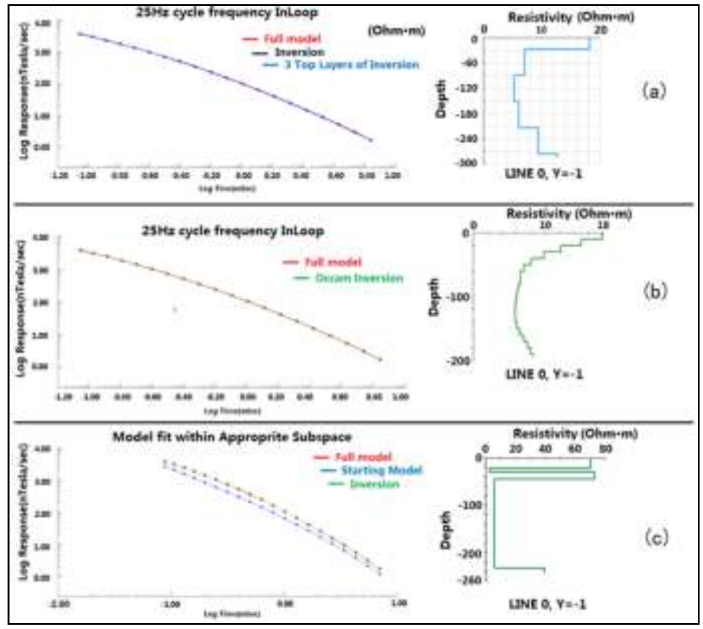

Fig. 4. Comparison of different inversion results

For inversion problems with many suitable models, it is standard theory to use additional data to find more unique models. For TEM soundings, it has become quite common to use multiple base frequencies in order to have more data available and to have more low frequency data in an attempt to derive better depth resolution. However, if using the same instrumentation there will be little variation in the decays except additional late time channels.

In the second simulation, we utilize a central loop measurement with an additional two measurements outside the loop. This is analogous to the step-wise moving loop technique (Powell et al, 2007) adopted in the Canadian Athabasca basin for uranium exploration. In the first example, we use no a priori information but rather a uniform half-space starting model. Figure 6 shows results utilizing multiple data points. In Figure 6a, we see at the top the configuration, the loop red and the 3 stations as blue triangles. The 3 plots, below, are all of Hz, at the three station locations. Model results for a single inversion utilizing the data for 3 stations are plotted as well for each location.

For Figure 6(a), we use as a starting model, 4 layers plus a half-space with all layers having a resistivity of 100 and the top 4 layers equal thickness. From the inversion result, we can see that the approximate depth of top layer is found plus the average resistivity down to basement. The depth to the top layer is quite close, a conductive zone is found but the model misses the intermediate resistor although the depth to basement is quite close. This result indicates that 3 separations reduce the number of possible subspace model types but in this case even 3 separations are not sufficient for a precise resolution.

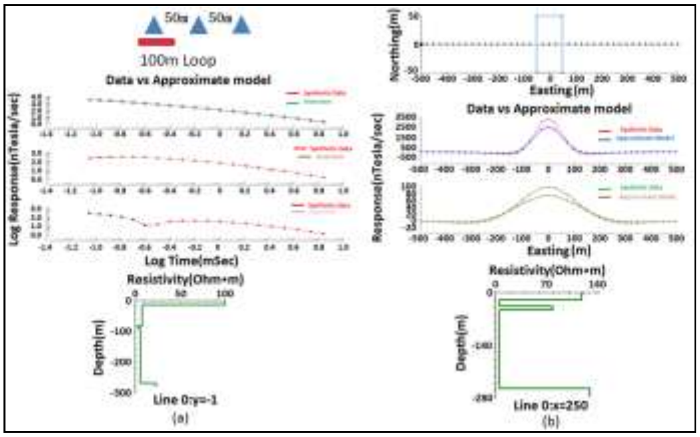

Fig. 5. Multiple Data Strategies

Figure 6(b) exaggerates this approach by utilizing many data stations. The first step is to find an approximate model by simple forward modelling to find a model which resembles Hz and Hx at all times. In Figure 6b we show the results of the approximate model at an early time channel and at a late time. The starting model is the approximate model and then the inversion begins from west inverting the first station and the inversion proceeds utilizing the previous inversion as a starting model. If the ground is approximately one dimensional and slowly varying then this approach is both effective and fast (Davis, 2009). This seems practical as we must assume that the lateral gradients in the ground resistivity are quite slow for any 1D inversion approach. The final results are show in Figure 7. The results are quite good implying that the non-uniqueness outside the loop is less severe than inside the loop.

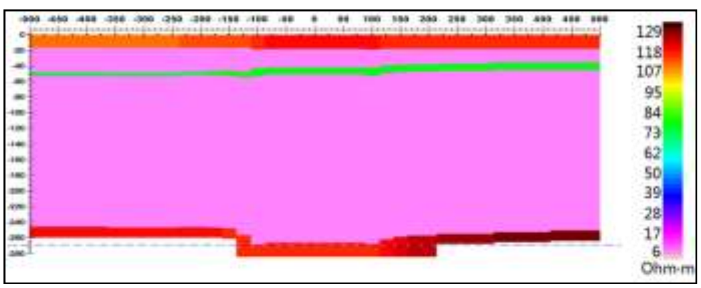

Fig. 6. Inversion Results for Fixed Loop survey

IV. Field Survey Examples

The synthetic studies are insightful but we must now consider practical issues regarding the theoretical work. While there have been numerous field surveys performed over the years (e.g. Powell et al, 2007, Davis and Groom, 2009, Dickenson et al, 2010), we devised a number of specific field tests which could be performed in a very favorable site. All the test surveys were carried out during May 28, 2015 and June 3, 2015. The purpose for these tests is to confirm those conclusions from our synthetic data. We surveyed in a very flat Gobi terrain filled with feathered volcanic gravel as the surface is flat and the stratigraphy is expected to be very flat. The geology and the survey configuration are shown in Figure 8.

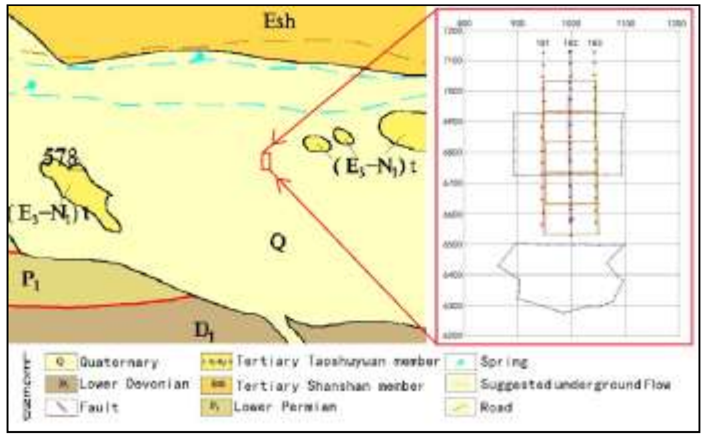

Fig. 7. Survey configuration map

This test site is located in the middle-south of the Hami basin, located between Kazakhstan plate, Siberia plate and Tarim plate. Three tectonic units exist in this basin: North depression, Lake Ayding slope and the Nan hu rise. Our working area is located in the north of Nan hu rise.

Three survey configurations were utilized. First, 3 profiles (L181, L82, L183) were measured from a single fixed loop. As part of a separate test, a ragged loop was used with 50m line spacing and 40m station spacing. The base frequency utilized was 25 Hz and all three components of the time varying magnetic field were measured utilizing a Geonics Protem receiver, 3D-3 coil sensor and an EM67 transmitter. Following this survey, a 200m x 200m loop was laid out in the center of the 3 profiles and again with 25Hz, 5 stations were measured on L182. Stations were located at 300m and 200m north and south from the loop center and at the loop center. Again, all 3 components are measured.

Finally, a moving loop configuration was utilized along L182. A square 100m loop was used and data were taken at the center of the loop, and 70m and 150m north of the center of the loop. 15 stations were measured with 3 components at 25Hz and 2.5Hz.

First we would like focus on fixed loop data since the fix loop data may tell us quickly for a large area if the resistivity structure is approximately 1D. If the ground is not approximately 1D, then in-loop data is almost certainly of little value and thus any 1D inversion based on in loop data is likely not representative of the ground structure. Figure 9 shows Hz and Hx which are representative of a current migration. Figure 9(a) presents the 3rd Hz channel, and Figure 9(b) the 9th channel. From this, we observe that there is a weak structure striking a few degrees south of EW. Figure 9(b) the 9th Hz channel, we can see quite clearly that the currents are not migrating uniformly with Y and there is a strong three-dimensional structure to the north. Figure 9(c) shows current migration of the

14th Hx channel and it shows very clearly a shallow structure near the loop as well as the northern structure.

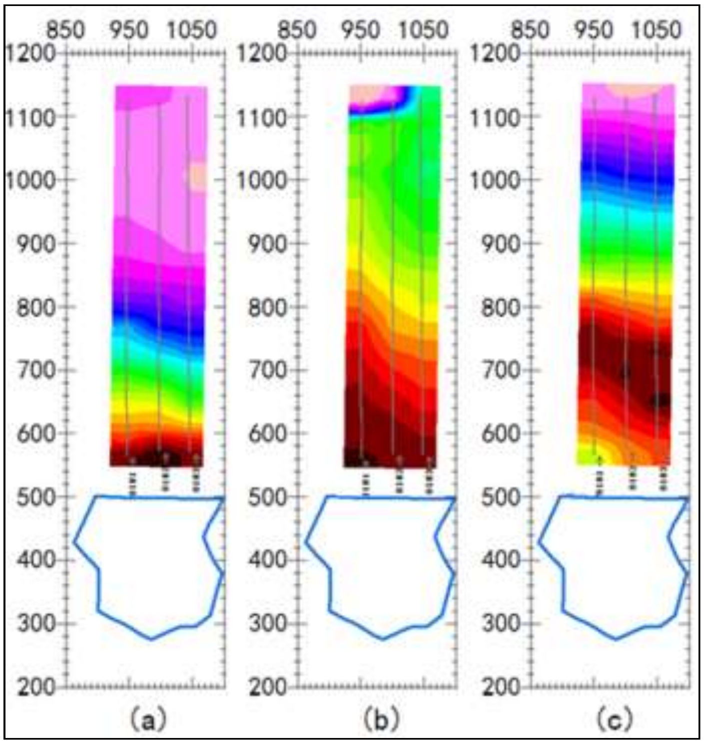

Fig. 8. Left to right, Hz Channel 3, 9 and Hx channel 14

Observation of the fixed loop data shows that the late time data does not conform to a 1D structure in the northern portions of the survey. Thus, we chose first chose to invert for a 1D inversion model using the first 8 time channels of Hz with the model to fit the data 12 stations nearest the loop. Figure 10 displays the results. Figure 10(a) is the Hz channel 2 inversion result and we observe that the data in this manner is quite sensitive to both the top and 2nd layer resistivity as well as the thickness of the top layer. However, we can see the lack of 1D response in Hz out a few hundred meters from the loop as well as in Hy. The same situation appears in Hz channel 6 (Figure 10(b)). The model fits Hz fit quite well but we can start to see the response from a 3D structure near the end of the line. The final model is 142 Ohm-m with a thickness of 68m, 410 Ohm-m with a thickness of 538m and underneath a very strong resistor. However, the resistor has very little effect on the synthetic data due to its depth.

Figure 11 displays the inversion results of data from Stn 6630 from the 200m loop. The 3 southern stations were jointly inverted for one model. Only Hz was used in the inversion and all the time channels except the first and the last were utilized.

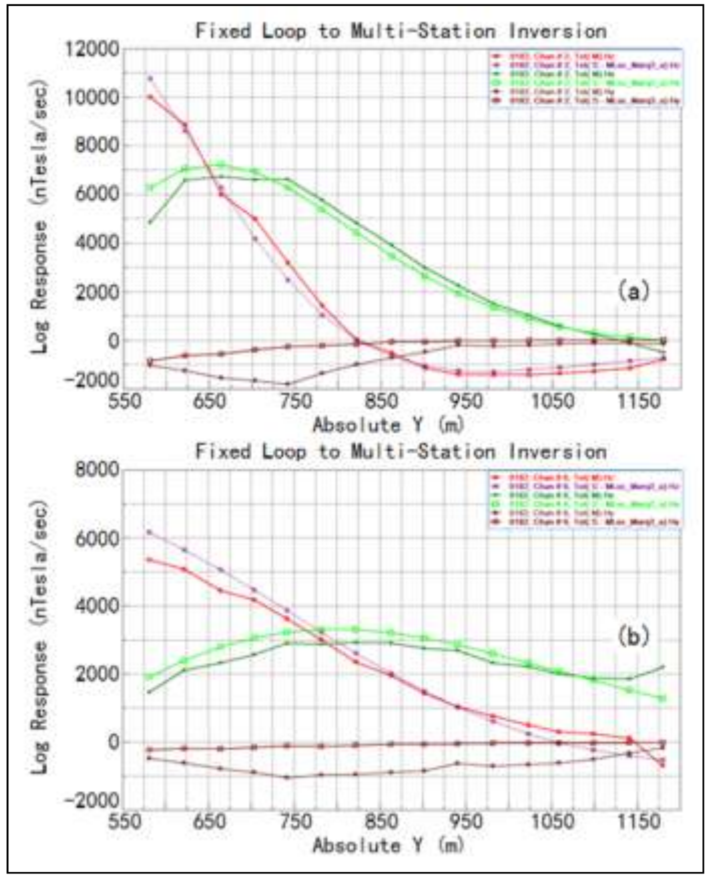

Fig. 9. Fix loop Hz data modeling result

Initially, a 5 layer over a half-space was used but this produced essentially a layer over a half-space result. The model is simply 220 Ohm-m for 525m and then a resistor. The data is unable to resolve either a difference in resistivity in the upper 500m however depth to a resistor is quite well resolved and the resistivity of this resistor must be over 2000 Ohm-m. We could not find a 1D model that fit for the 4th station from the north, both for Hz and Hx, indicating that these stations are sensitive to the 3D structure to the north as observed in the fixed loop data.

For the 100m moving loop data, we will first examine the 2 southern loops; Loop 1 and Loop 2. Inversion results are shown in Figure 12. Recall the 3 station inversion for the 200m loop: 220 Ohm-m for 530m with 8000 Ohm-m below. The difference for these 2 100m loops is that the top layer is divided into an upper portion somewhat more conducting than 220 and a lower section somewhat more resistive. This feature cannot resolve by 200m loop.

Figure 12(a) shows a comparison of in-loop data to 3 station inversion from 200m loop. The 200m loop model is relatively close but the in-loop measurement indicates that there is a more conducting top than 220Ohm-m and then and intermediate more conducting zone followed by the resistive basement.

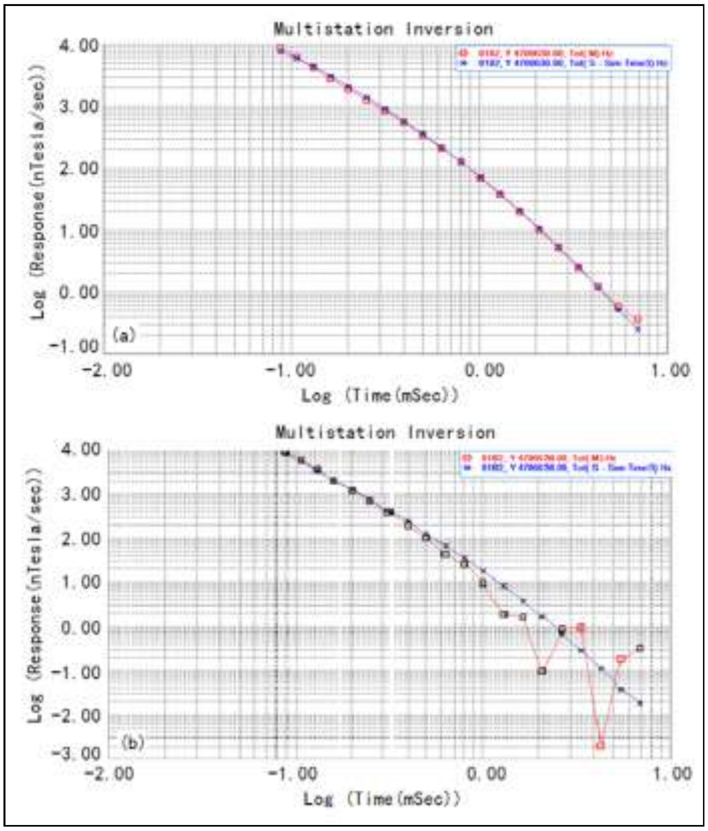

Fig. 10. Inversions results, Station 6630 - 200m loop

Figure 12(b) shows a comparison of 70m data to 3 station inversion from 200m loop. The 200m loop model is relatively close but the 70m measurement indicates that 220 Ohm-m is about the average and the depth is approximately correct to the resistor but the resistor is too great. Figure 12(c) shows a comparison of 150m data to 3 station inversion from 200m loop. The 200m loop model is also very close for the 150m measurement but there is still the indication that the top layer of our model is divided into a top section somewhat more conducting.

We have shown that the 3 separations are consistent but the inloop data does not recognize the division in the top layer as well as the 70m and 150m measurements. We will continue by examining attempting to invert the data. We first inverted Hz at the center of the loops and found our best model to be 38 Ohm-m for 13m followed by 1230 Ohm-m for 145m with 240 Ohm-m below. Figure 13(a) shows a fit of Hz to 3-layer model in-loop. The fit is relatively good down to Ch15. Figure 13(b) shows a comparison of Hz to 4 layer in-loop inversion for 150m separation. The in- loop inversion does not appear to resolve the conductivity of the 3rd layer well. Figure 13(c) shows a comparison of Hx to a 4 layer in-loop inversion for 150m separation. Though affected by noises beyond Chn7, Hx still can explain this issue.

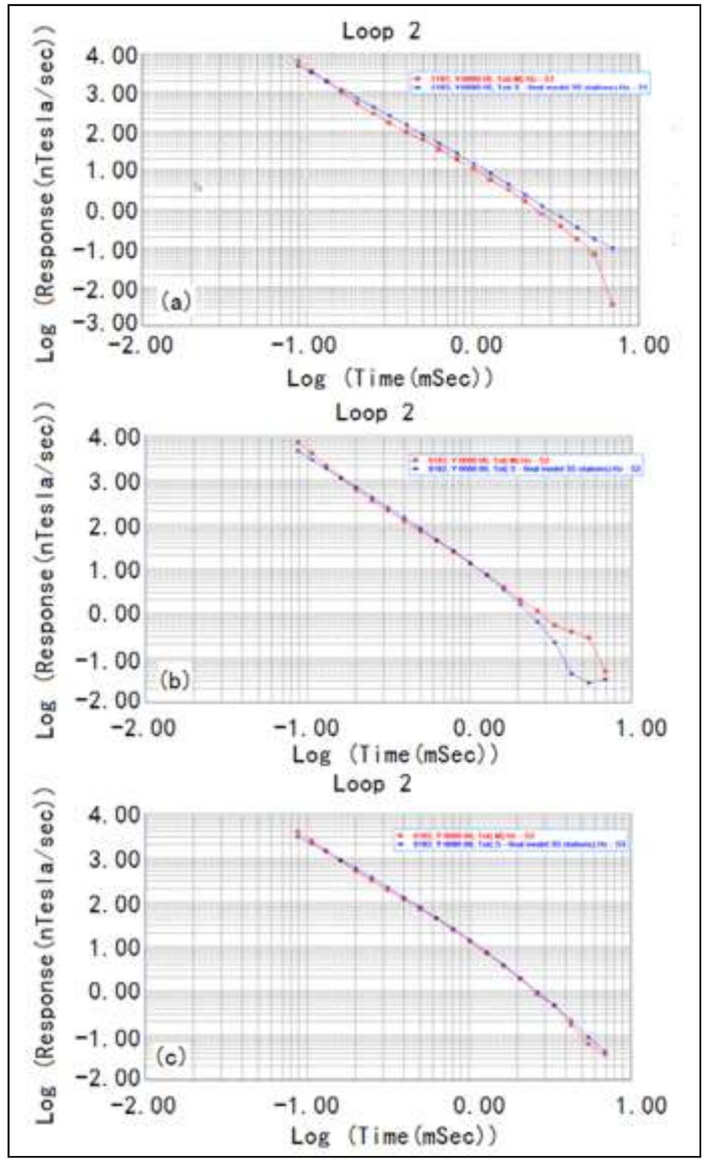

Fig. 11. Modeling results from 3 separations of loop 2

With a combination of all 3 separations we are able to give our best fitting model for moving loop data, 37 Ohm-m with a thickness of 13m, 3920 Ohm-m with a thickness of 35m, 1300 Ohm-m with a thickness of 162m, 195 Ohm-m with a thickness of 532m then a resistor. Modeling result is shown in figure 14.

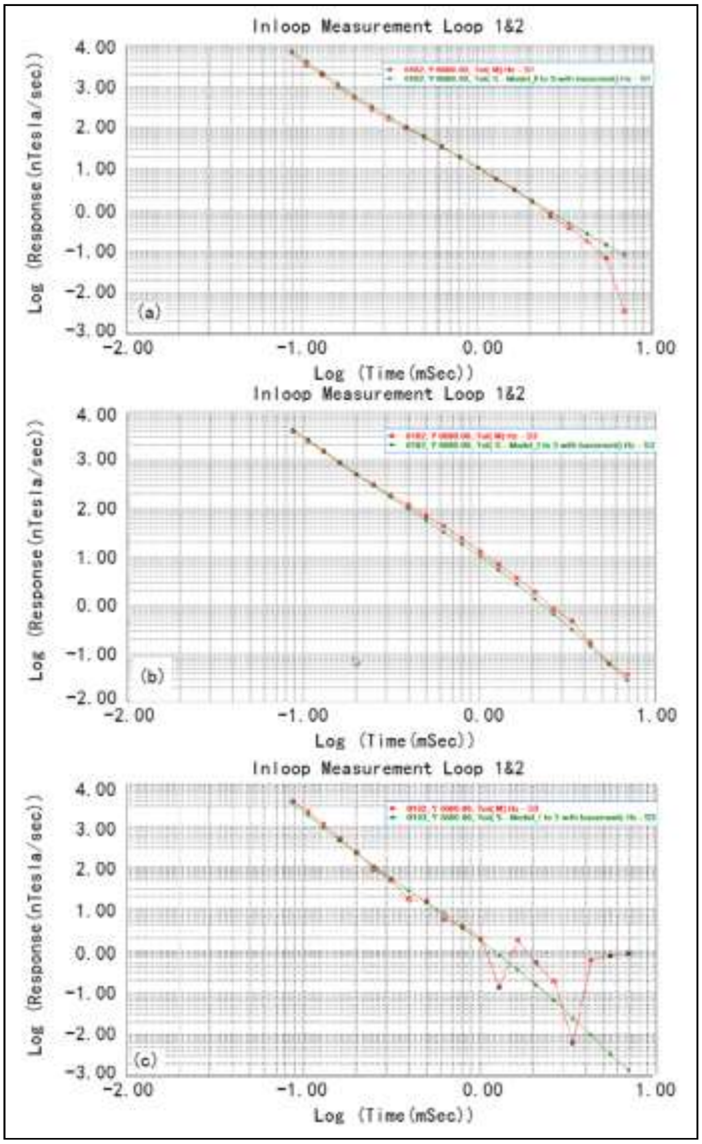

Fig. 12. Comparison between in-loop and 150m data from loop 2

V. Conclusions

From this study we discovered that inversion of in-loop data is dangerous as this location is poor for sensing the response of the ground. If the ground is not approximately 1D, then in-loop data misrepresents the true resistive structure. Measuring with a multiple separation strategy may increase the resolution and Hx can be utilized as and fewer models can fit all stations.

But this strategy still cannot provide a clear view of a large area as to whether the underground is approximately 1D. Fixed loop data gave us most information of the survey area: a) The earth is mainly 1D at shallow depths because all 3 lines and all 3 components match a single model. b) There is a strong 3D structure at the north end of the lines; all 3 components are strongly sensitive to this structure. c) There is a weak structure near the loop. All 3 components are sensitive but Hx is easiest to diagnose. So fixed loop data is reasonably reliable no matter of data quality and also in consideration of working efficiency.

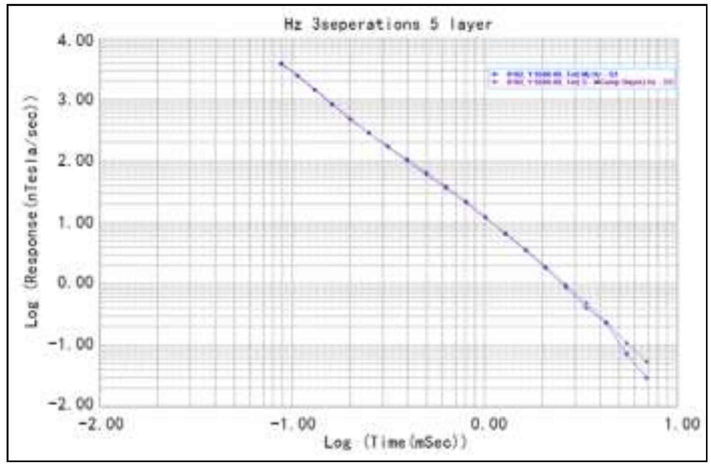

Fig. 13. A combinations of 3 separations modeling result

References

[1] Anderson, W.L., 1975, Improved digital filters for evaluating Fourier and Hankel transform integrals, U.S. Dept of Commerce, National Technical Information Service Report PB-242-156

[2] Anderson, W.L., 1982, Fast Hankel transforms using related and lagged convolutions: ACM Trans. On Math. Software, 8, 344-368

[3] Anderson, W.L., 1993, Interactive inversion of transient electromagnetic data for a central-induction loop over layered earth models V1; U.S. Geological Survey Open-File Report, 93-234-A/B

[4] Boerner, D.E. and G.F. West, 1984, Efficient calculation of the electromagnetic fields of an extended source, Geophysics Vol. 49, p 2057-2060

[5] Johansen, H.K., and Sorensen, K., 1979, Fast Hankel transforms: Geophysical Prospecting, 27, 876-901

[6] Groom, R.W., 2000, FSEMTRS, an algorithm for frequency to time domain transformation, Internal Report and manual, available online, www.petroseikon.com

[7] Jia, R. and Groom, R.W., 2005, On Time-Domain Transient Soundings, Symposium on the Application of Geophysics to Engineering and Environmental Problems, pg 506-512

[8] Dickenson, J.E., Pool, D.R., Groom, R.W. and Davis, L.J., 2010, Inference of lithological distributions in an alluvial aquifer using airborne transient electromagnetic surveys, Geophysics V75, pgs 149-161

[9] Jia, R., Davis, L.J. and Groom, R.W., 2009, Some issue on 1D-TEM inversion utilizing various multiple data strategies, SEG Technical Program Abstracts 2009, pg 739-743

[10] Powell, B., Wood. G., and Bzdel, L., 2007, Advances in Geophysical Exploration of Uranium Deposits in the Athabasca Basin, 2007 Plenary Session: Ore Deposits and Exploration Technology, Toronto, Canada, pgs 771-789

[11] Davis, L.J. and Groom, R.W., 2009, A comparison of airborne and ground electromagnetic data near the Grand Canyon, SEG Technical Program Abstracts 2009, pgs 764-768